

Structural changes during severe hot forging of the aluminum alloy 1570C

O.S. Sitdikov^{1,†}, R.N. Garipova^{1,2}, E.V. Avtokratova¹, O.E. Mukhametdinova¹,
M.V. Markushev¹

[†]sitdikov.oleg@anrb.ru

¹Institute for Metals Superplasticity Problems RAS, Khalturin St. 39, 450001 Ufa, Russia

²Ufa State Aviation Technical University, 12 K. Marx St., Ufa, 450000, Russia

Microstructure evolution in the ingot of Al-Mg-Sc-Zr alloy 1570C during multidirectional forging (MDF) to the strain 10.5 at 450°C ($\sim 0.77 T_m$) and 10^{-2} s^{-1} was investigated. The alloy belongs to advanced structural materials exhibiting high strength at ambient temperature. It can be easily hot worked, demonstrates superior superplasticity in a fine-grained state, while its cold deformation is limited due to high yield-stress and relatively low ductility. Consequently, an evaluation of grain refinement potentiality in this alloy at high temperatures may be important for industrial application. Before MDF, the alloy had the equiaxed grains $\sim 25 \mu\text{m}$ in size with near uniformly distributed nanoscale coherent dispersoids $\text{Al}_3(\text{Sc,Zr})$. In the early MDF stages, new fine (sub)grains with low- and high-angle boundaries were formed near original grain boundaries. With increasing strain, the fraction of these crystallites increased, finally resulting in almost fully recrystallized structure with grain size $\sim 3 \mu\text{m}$ and fraction of high-angle boundaries (HABs) ~ 0.9 . The strain dependency of microstructural parameters showed that grain refinement occurred mainly via continuous dynamic recrystallization. There was a strong interaction between lattice dislocations, (sub)grain boundaries and coherent dispersoids $\text{Al}_3(\text{Sc,Zr})$. This implies that the latter effectively hindered (sub)grain boundary migration and provided dislocation accumulation, resulting in formation of high-density subboundaries and their transformation into HABs, even at high temperatures. Moreover, hot MDF did not lead to any degradation of the alloy high strength. The data obtained have shown that there was a great potential for extensive grain refinement in this alloy at elevated temperatures alleviating difficulties of its thermo-mechanical processing.

Keywords: aluminum alloy, multidirectional forging, microstructural evolution, continuous dynamic recrystallization.

Структурные изменения в процессе горячей всесторонней ковки алюминиевого сплава 1570С

Ситди́ков О.Ш.^{1,†}, Гари́пова Р.Н.^{1,2}, Автокра́това Е.В.¹, Мухаме́тдинова О.Э.¹,
Марку́шев М.В.¹

[†]sitdikov.oleg@anrb.ru

¹Институт проблем сверхпластичности металлов РАН, ул. Ст. Халтурина 39, 450001, Уфа, Россия

²Уфимский государственный авиационный технический университет, ул. К. Маркса 12, Уфа, 450000, Россия

Исследована эволюция структуры в литом Al-Mg-Sc-Zr сплаве 1570C при всесторонней изотермической ковке (ВИК), до степени деформации 10,5 при 450°C ($\sim 0.77 T_m$) и 10^{-2} c^{-1} . Данный сплав является перспективным конструкционным материалом, обладающим высокой прочностью при комнатной температуре. Он может легко деформироваться при повышенных температурах, в мелкозернистом состоянии демонстрирует высокие сверхпластические свойства, в то время как холодная деформация вызывает ряд проблем из-за высоких напряжений течения и сравнительно низкой пластичности. Соответственно, оценка потенциала измельчения зерен в данном сплаве при высоких температурах является важной для его промышленного применения. Перед ВИК сплав имел равноосную зеренную структуру с размером зерна $\sim 25 \text{ мкм}$ и равномерным распределением когерентных наноразмерных дисперсоидов $\text{Al}_3(\text{Sc,Zr})$. На ранних стадиях ВИК области новых мелких (суб)зерен, окруженных мало- и высокоугловыми границами, формировались вдоль исходных границ, а затем с увеличением степени деформации объемная доля этих кри-

сталлитов увеличивалась, приводя к формированию микроструктуры со средним размером мелких зерен ~ 3 мкм и долей высокоугловых границ $\sim 0,9$. Характер зависимости параметров формирующейся микроструктуры от степени деформации показал, что измельчение зерен осуществлялось в соответствии с непрерывной динамической рекристаллизацией. Выявлено сильное взаимодействие между решеточными дислокациями и/или границами (суб)зерен и наноразмерными частицами $Al_3(Sc,Zr)$. Это означает, что дисперсные частицы могли даже при повышенной температуре эффективно сдерживать миграцию границ зерен, а также обеспечивать накопление дислокаций, ведущее к формированию субграниц высокой плотности и их трансформации в большеугловые границы. Также показано, что ВИК не приводила к деградации высоких прочностных свойств сплава. Полученные данные свидетельствуют в пользу того, что имеется большой потенциал для интенсивного измельчения зерен сплава при повышенных температурах, облегчающих его термомеханическую обработку.

Ключевые слова: алюминиевый сплав, всесторонняяковка, эволюция микроструктуры, непрерывная динамическая рекристаллизация.

1. Introduction

Processing bulk ultrafine-grained (UFG) materials with the grain size $\leq 1 \mu m$ in the thermo-mechanical treatment involving severe plastic deformation (SPD) acquired a great interest from the researchers in the field of material science and solid state physics owing to achieving enhanced combination of physical and mechanical properties [1–16]. Several SPD techniques, such as equal channel angular pressing [1–3, 7–15], accumulative roll bonding [2,4,11] and multidirectional forging (MDF) [1,2,6,9–11] are often used to produce the UFG structures. Besides, these techniques can be employed as effective “scientific tools” that allow investigating the structural changes at large strains [1, 4–7, 10,12–14].

Currently, the characteristics of various SPD methods as well as the properties of semi-finished products with UFG structures are fairly well studied [1,2,7,9,11]. Among the materials with high stacking fault energy, a respectable number of studies were addressed to analysis of regularities of UFG structure formation in Al alloys at low and medium deformation temperatures ($< 0.5 T_m$, where T_m is a melting point of aluminum). It has been shown [6–9,12–14] that the grain refinement in Al alloys during SPD may be related to the formation of dislocation subboundaries with low- and moderate (up to 15°) misorientation angles at comparatively low strains. With further straining, the number and misorientation of these boundaries increased leading to the formation of UFG structure with large fraction of high-angle ($\geq 15^\circ$) boundaries (HABs). Such process of new ultrafine grain formation was associated with continuous dynamic recrystallization (cDRX) [5,6,8,10,12–14]. However, in the overwhelming majority of works, the detailed studies of the microstructural development during SPD of Al alloys were mainly limited by temperature range from ambient to $\sim 200–250^\circ C$ [1,3,4,7,8,12–14]. The occurrence features of this grain refinement mechanisms (and even the possibility of their realization) at higher temperatures still remain undisclosed. This, in particular, is quite important for some heavily alloyed high-strength Al alloys, whose plastic deformation is frequently accompanied by the premature failure at low and intermediate temperatures, which does not allow high strains in the SPD process [12,14].

The aim of this study was the analysis of the evolution of structure in commercial cast and homogenized alloy 1570C subjected to MDF at $450^\circ C$ ($\sim 0.77 T_m$) to elucidate

the feasibility of obtaining UFG structure. The alloy belongs to advanced structural materials exhibiting high strength at room temperature. It can be easily hot worked, while cold forming causes problems because of high yield stress and relatively low ductility and toughness.

2. Material and procedure

The material used was commercial Al alloy 1570C with the following chemical composition: Al-5%Mg-0.18%Mn-0.2%Sc-0.08%Zr (in wt.%). The ingot fabricated by direct chill casting was homogenized at $350^\circ C$ for 6h. Rectangular samples of 18 mm (X) \times 17 mm (Y) \times 10 mm (Z) were machined from the ingot supplied. Three-directional multi-pass compression was carried out at a strain rate of $10^{-2} s^{-1}$ under isothermal conditions at the temperature of $450^\circ C$ with changing in the loading direction of 90° from pass to pass, to provide data compatible with those represented in [6,10]. The total strain $\varepsilon = \Delta\varepsilon_1 + \Delta\varepsilon_2 + \Delta\varepsilon_3 + \dots + \Delta\varepsilon_n$, where $\Delta\varepsilon_n = 0.7$ was the true (logarithmic) strain in each compression pass, was applied to 10.5. The samples were quenched in water after each pass, then reheated to deformation temperature and kept for about 5–10 min before subsequent deformation. A colloidal graphite powder was used as a lubricant.

The microstructural analysis was carried out in the central part of specimens deformed to various strains in a section parallel to the last compression axis. Metallographic observations were carried out using a Nikon L-150 optical microscope after etching of the samples with a standard Keller's reagent. Orientation imaging microscopy (OIM) maps and misorientation distributions of the (sub)boundaries were obtained by electron back scattering diffraction (EBSD) analysis using a TESCAN MIRA 3 LMH scanning electron microscope (SEM) equipped with a field-emission gun and the Oxford Instruments- HKL Channel 5 system. In the EBSD maps represented, the different colors indicated the different crystallographic orientations and the orientation differences (θ) between neighboring grid points, $2^\circ \leq \theta < 15^\circ$ (low angle boundaries) and $15^\circ \leq \theta \leq 62.8^\circ$ (high-angle boundaries) were marked by light-gray, and black lines, respectively. Transmission electron microscopy (TEM) was performed using a JEOL-2000EX TEM. Specimens for TEM and SEM examinations were electro-polished at 20 V in a solution of 30% HNO_3 and 70% CH_3OH at a temperature of $-28^\circ C$ in a Tenupol-5 twin-jet polishing unit. The average size of strain-induced (sub)grains was evaluated by an equivalent

diameter technique (as an equal-area circle diameter for an ellipse fitted on (sub)grain). The Vickers microhardness (HV) at room temperature was measured using the standard procedure and a load of 0.5 N.

3. Results and discussions

Initial structure. After homogenization, the as-cast alloy had an equiaxed grain structure along with precipitates formed, as shown in Fig. 1. Fig. 1a represents the typical grain structure with the average grain size of $\sim 25 \mu\text{m}$ and a small amount of remnant particles of excess phases that were emerged from the melt upon solidification [16]. These particles were distributed at grain boundaries, as well as at some triple points. Homogeneous spatial distribution of nanosized coherent dispersoids of $\text{Al}_3(\text{Sc,Zr})$ phase with relatively weak diffraction contrast was revealed by TEM examination (as arrowed in Fig. 1b).

A typical microstructure after MDF to $\varepsilon = 10.5$ is represented in Fig. 2. It is seen that hot MDF led to a considerable grain refinement. Namely, about 80–90% of the deformed material were occupied by new fine grains that appeared in dark-color regions in Fig. 2a, though some remnant original grains (white-color regions in Fig. 2a) still existed even at such high strain. The size of the crystallites evolved in fine grain regions was about $3 \mu\text{m}$, as shown in the EBSD map in Fig. 2b obtained at larger magnification. Thus, it is evident in Fig. 2 that there is a feasibility to produce almost fully developed fine-grain structure in the present alloy by MDF at 450°C .

Microstructural evolution during MDF is presented in Figs. 3–5 showing typical EBSD (Fig. 3) and TEM (Figs. 4–5) structures developed at various strains. It can be seen (Fig. 3) that in the early stages of MDF, original coarse grains changed periodically their shape (Figs. 3a–c).

Concurrently, the areas of new fine (sub)grains, surrounded by low- and high angle boundaries, were formed in the mantle regions of these grains followed by their propagation toward the interiors of original grains (Figs. 3c,d). The volume fraction of these crystallites gradually increased in the course of MDF from 0.09 ($\varepsilon = 2.1$) to 0.81 ($\varepsilon = 6.3$) and the majority of strain-induced boundaries achieved the high-angle misorientation, leading to the recrystallized structure with high HABs fraction.

TEM analysis (Fig. 4) showed that the most of (sub)grains developed at $\varepsilon = 2.1$ (see Fig. 4a) had a non-equilibrium shape and were bonded by the dislocation boundaries with the non-uniform extinction contrast. The structure inside

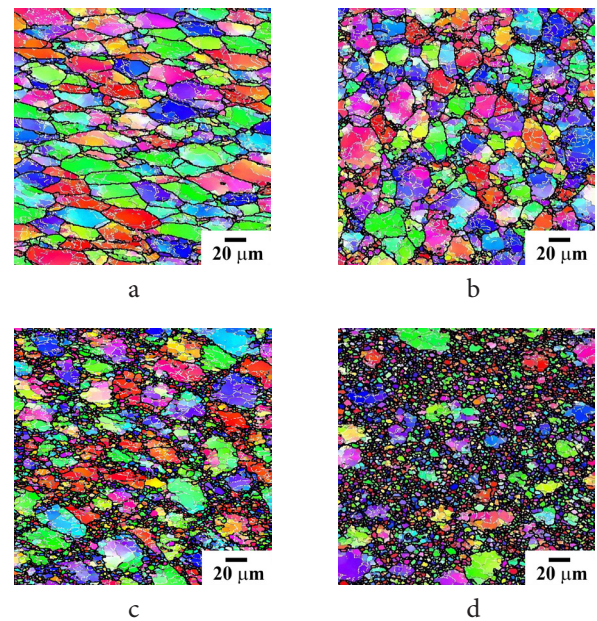


Fig. 3. (Color online) EBSD maps of the 1570C alloy after MDF: (a) $\varepsilon = 1.4$; (b) $\varepsilon = 2.1$; (c) $\varepsilon = 4.2$; (d) $\varepsilon = 6.3$.

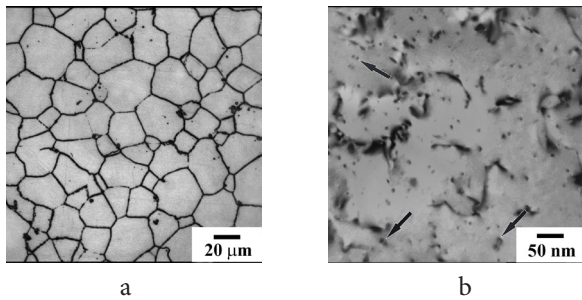


Fig. 1. Microstructure of the homogenized 1570C alloy (a) optical microscopy; (b) TEM.

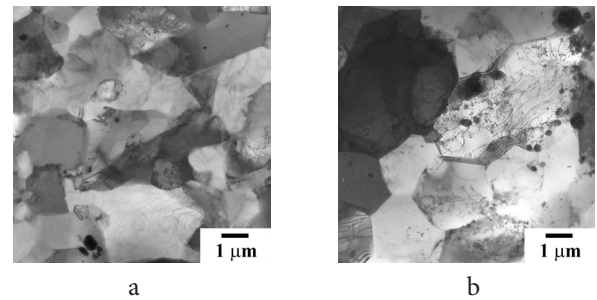


Fig. 4. TEM structures of the 1570C alloy after MDF: (a) $\varepsilon = 2.1$; (b) $\varepsilon = 10.5$.

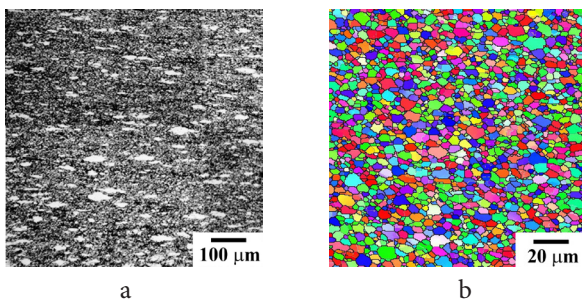


Fig. 2. (Color online) Microstructure of the 1570C alloy after MDF to $\varepsilon = 10.5$: (a) optical microscopy; (b) EBSD. Hereafter, the last compression axis is vertical.

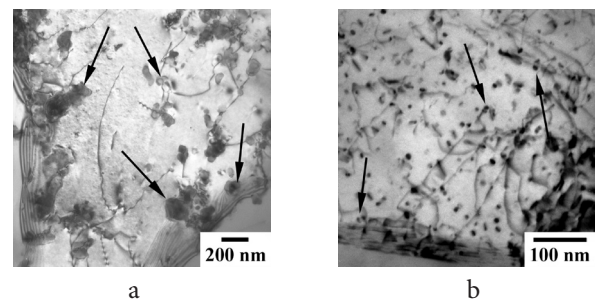


Fig. 5. Distribution of dispersion particles in the 1570C alloy after MDF to $\varepsilon = 6.3$. Coarse and fine $\text{Al}_3(\text{Sc,Zr})$ particles are arrowed in (a) and (b), respectively.

(sub)grains was characterized by a relatively low density and heterogeneous distribution of lattice dislocations. At high strain, $\varepsilon = 10.5$, more uniform and equilibrium structure, having (sub)grain boundaries with the angles at triple junctions of near to 120° , was commonly formed (Fig. 4b).

Fig. 5 demonstrates the TEM images of the $\text{Al}_3(\text{Sc,Zr})$ precipitates in fine (sub)grains developed in the samples underwent MDF to $\varepsilon = 6.3$. Both the particles and individual dislocations, pinned by them, were revealed. Besides, a strong mutual interaction between particles and (sub) grain boundaries can be noticed in the images. Most likely, the precipitates that are served as the strong pinning agents in the present alloy [6,10,12,14,16] could restrict the dislocation climb (and their rearrangement) on the long distances and so, prevent their annihilation under high-rate dynamic recovery conditions. Also the strong limitation for the grain growth could take place owing to interaction of grain boundaries and dispersoids. Those may be the main factors responsible for occurrence of grain refinement and development of very fine grain structure even at such high temperature as 450°C (Fig. 2) [12]. At the same time, it should be noted that the morphology of the particles in the grain interiors and in the regions adjoining the grain boundaries was clearly different. While the clusters of very fine coherent particles, having a weak diffraction contrast, were mainly observed in the grain interiors (see the center of Figs. 5a and b), much coarser precipitates were present in some grain boundary regions (Fig. 5a). The latter had a globular compact shape and much larger size and some of them lost their coherency with the surrounding aluminum matrix. This suggested that intense coarsening of the precipitates took place in the vicinities of the grain boundaries upon a high temperature straining. The reasons for such rapid particle coarsening were discussed in detail elsewhere [16]. The most common ones may be the loss of coherency of the particles upon their interaction with the grain boundaries, as well as the enhanced diffusivity of Sc- and Zr- dissolved atoms along high-angle boundaries, as it can be compared with the grain interiors.

Microstructure parameters. Fig. 6 represents changes in the misorientation distributions of deformation-induced (sub)grain boundaries derived from EBSD analysis. It is seen (Fig. 6a) that almost all intercrystallite boundaries in the initial as-cast structure were high-angle ones. Most of the boundaries ($> 60\%$) developed at the early stages of MDF (Fig. 6b) exhibited low-to-medium angle misorientations from 2 to 15° , while those above 15° were inherited mainly from the initial structure (see Figs. 3a,b). With further straining (Figs. 6c–e), the fraction of low and moderate angle boundaries rapidly decreased and that of high-angle ones conversely increased owing to development fine-grained regions (see Figs. 3c,d) and so, this may be directly associated with formation of new fine grains. Noteworthy that the average misorientation of 36.5° in the newly evolved structure at $\varepsilon = 10.5$ (Fig. 6e) is less than that of 40.7° , predicted by Mackenzie for randomly misoriented polycrystalline aggregates of cubic metals [17]. This difference may be attributed to the feature of the strain-induced microstructure, in which a fraction of low- angle boundaries is always present [6,10].

Strain dependencies of (a) the average misorientation, Θ_{ave} , and (b) the fraction of HABs, f_{HABs} , are depicted in Fig. 7. As seen, both Θ_{ave} and f_{HABs} varied with strain in a complex manner. Namely, in the original material state, they were 39.5° and 0.92, respectively, but, at small MDF strains, low-angle boundaries were formed and these parameters decreased to about 15° and 0.35 at $\varepsilon = 1.4 - 2.1$. However, new grains were developed continually with strain, as shown above. Therefore, both angular parameters increased at larger strains, tending to reach the values about 36.5° and 0.88 at $\varepsilon = 10.5$, correspondingly, that are only a bit smaller than those of the non-deformed material.

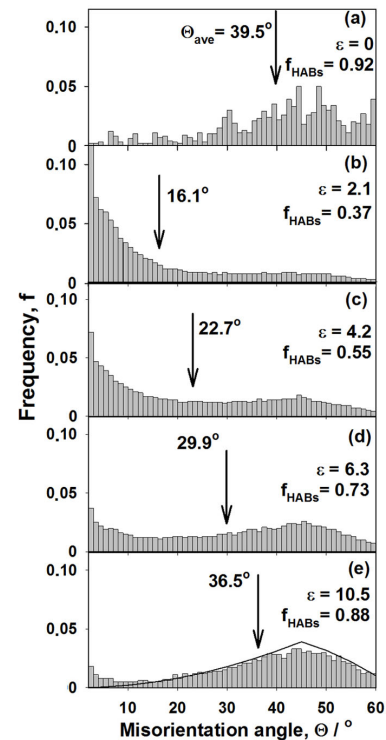


Fig. 6. Misorientation distribution for (sub)grain boundaries developed in the 1570C alloy after MDF to various strains. Solid line shows Mackenzie distribution.

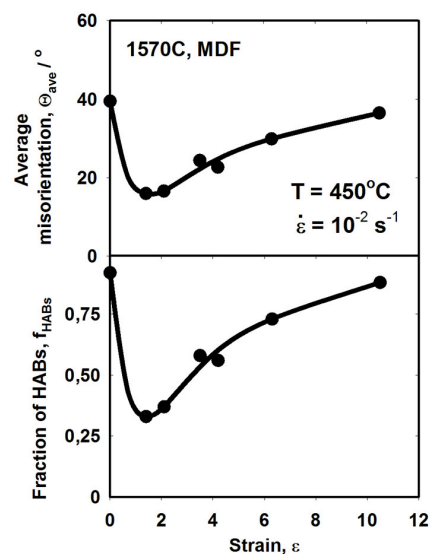


Fig. 7. Strain dependencies of the angular microstructural parameters, Θ_{ave} and f_{HABs} developed in the 1570C alloy after MDF.

The average sizes of (i) subgrains, d_{sg} , derived from the EBSD analysis and defined as sizes of crystallites surrounded by all intercrystallite boundaries from 2° ; and (ii) fine grains, d_{FG} , defined as the sizes of crystallites in the fine-grained regions, bonded by the boundaries with misorientations from 15° , are shown vs ε in Fig. 8. It is seen that the d_{FG} monotonically decreased to $\sim 2.5 \mu\text{m}$ during MDF to $\varepsilon = 4-6$ and then slightly increased to $\sim 3.0 \mu\text{m}$ at $\varepsilon = 10.5$; that may be attributed to the coarsening of dispersoids at higher strains. It is also evident that the (sub)grain size obtained after moderate-to-large strains is of the order of the crystallite size observed by TEM (Fig. 4). Referring to almost the same (sub)grain size developed (Fig. 8), as well as progressive increase in misorientation and fraction of HABs during deformation (Fig. 7), such process of microstructure evolution can be mainly categorized as cDRX [5,6,10,14,18].

Microhardness changes vs strain are shown in Fig. 9. It is important to note that the alloy did not generally lose its high strength after high-temperature thermo-mechanical treatment. That probably was mainly attributed to the fact that a large fraction of dispersed particles still insisted to remain coherent, nano-dispersed and uniformly spatially distributed in the grain interiors (see Fig. 5b). Second, a softening effect from a particle coarsening would be also somewhat compensated by the strengthening owing to grain refinement during MDF. It should be noted that the deformed structures are varied in that case in accordance with a total strain (see Fig. 3), but equilibrium between crystalline defects induced by plastic working and those disappeared by some restoration (recovery) processes is reached to be responsible for constant flow stresses. Note that such strengthening behavior of the microstructure processed by hot MDF in the present Al alloy can be similar to that of some cubic materials subjected to SPD at low-to-moderate temperatures (e.g. [12,14]).

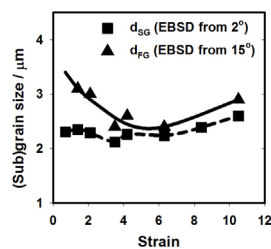


Fig. 8. Strain dependences of the size of fine (sub)grains developed in the 1570C alloy in MDF.

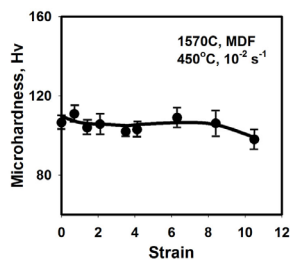


Fig. 9. Room temperature microhardness changes in the 1570C alloy depending on MDF strain.

4. Conclusions

A fairly fine grain structure with the grain size $2.5-3.0 \mu\text{m}$ may be introduced into a complex-alloyed hard-to-deform alloy 1570C even at the MDF temperature $0.77 T_m$ without any significant loss in its room temperature strength. This implies that there is a big potential for obtaining fine grain size in this alloy at high temperatures alleviating the difficulties of its processing. The strain dependency of the microstructural parameters suggests that the alloy grain refinement during hot MDF occurred mainly in accordance with cDRX.

Acknowledgments. This work was supported by the Russian Foundation for Basic Research (RFBR) under grant № 16-08-01189 A.

References

1. F. J. Humphreys, P. B. Prangnell, J. R. Bowen, A. Gholinia, C. Harris. Phil. Trans. R. Soc. Lond. A357, 1663 (1999).
2. R. Z. Valiev, R. K. Islamgaliev, I. V. Alexandrov. Prog. Mater. Sci. 45, 103 (2000).
3. A. Yamashita, D. Yamaguchi, Z. Horita, T. G. Langdon. Mater. Sci. Eng. A287, 100 (2000).
4. N. Tsuji, Y. Ito, Y. Saito, Y. Minamino. Scripta Mater. 47, 893 (2002).
5. F. J. Humphreys, M. Hatherly. Recrystallization and Related Annealing Phenomena, 2nd ed. — Amsterdam: Elsevier. 2004. 658 p.
6. O. Sh. Sitdikov, T. Sakai, A. Goloborodko, H. Miura, R. Kaibyshev. Philos. Mag. 85, 1159, (2005).
7. R. Z. Valiev, T. G. Langdon. Prog. Mater. Sci. 51, 881 (2006).
8. I. Mazurina, T. Sakai, H. Miura, O. Sitdikov, R. Kaibyshev. Mater. Sci. Eng. A473, 297 (2008).
9. R. R. Mulyukov, A. A. Nazarov, R. M. Imaev. Russian Physics Journal. 51, 492 (2008).
10. T. Sakai, H. Miura, A. Goloborodko, O. Sitdikov. Acta Mat. 57, 153 (2009).
11. M. V. Markushev. Letters on Materials. 1,36 (2011). (in Russian).
12. O. Sitdikov, E. Avtokratova, T. Sakai, K. Tsuzaki. Met. Mat. Trans. A 44, 1087 (2013).
13. S. Subbarayan, H. J. Roven, Y. J. Chen, P. C. Skaret. Int. J. Mater. Res. 104, 630 (2013).
14. O. Sitdikov, E. Avtokratova, T. Sakai. Journal of Alloys and Compounds. 648, 195 (2015).
15. M. H. Shaeri, M. Shaeri, M. Ebrahimi, M. T. Salehi, S. H. Seyyedein. Prog. in Nat. Sci.: Mat. Internat. 26, 182 (2016).
16. E. Avtokratova, O. Sitdikov, O. Mukhametdinova, M. Markushev, S. V. S. N. Murty, M. J. N. V. Prasad, B. P. Kashyap. Journal of Alloys and Compounds. 673, 182 (2016).
17. J. K. Mason, C. A. Schuh. Acta Mater. 57.14, 4186 (2009).
18. O. Sitdikov, R. Kaibyshev. Mater. Sci. Eng. A328, 147 (2002).